JOURNAL OF SPACECRAFT AND ROCKETS
Vol. 55, No. 3, May–June 2018

Conceptual Design of an Air-Breathing Electric Thruster for CubeSat Applications

Stephen W. Jackson* and Robert Marshall†
University of Colorado, Boulder, Colorado 80305

DOI: 10.2514/1.A33993

The altitude range between 120 and 300 km is relatively unexplored with regard to space weather, atmospheric models, climate observations, the global electric circuit, remote sensing, and intelligence gathering. This is due to the high magnitudes of drag experienced at these altitude ranges for any size of satellite. Air-breathing electric propulsion systems have been proposed for 50–100 kg satellites as a way to counteract drag at these altitudes. In this paper, a concept for an air-breathing ion thruster is designed for use in 3U, 6U, 12U, and 27U CubeSats. This design focuses on particle capture efficiency via a unique inlet design, the ionization efficiency of atmospheric particles, and then analysis of the thrust, taking into account those efficiencies. This work shows that it is possible to build air-breathing propulsion systems for CubeSats with thrust exceeding the local drag in low-Earth-orbit altitudes.

Nomenclature

A	=	area, m^2
C_D	=	coefficient of drag
D	=	drag, N
I_b	=	beam current, A
m_i	=	ion mass, kg
q	=	charge, C
T	=	thrust, N
T_g	=	grid transparency
V_b	=	beam voltage, V
v	=	velocity, m/s
v_a	=	acoustic velocity, m/s
v_g	=	velocity through the gap, m/s
ρ	=	density, kg/m^3

I. Introduction

THE region of the atmosphere and ionosphere between 120 to 300 km is relatively unexplored: the altitudes are too high for balloons or aircraft, but the drag is too high for spacecraft to remain in orbit for long. As such, the region suffers scientifically from a lack of in situ measurements. CubeSats have the potential to be a cost-effective platform to observe this region of the atmosphere if they can be equipped with a propulsion system to counteract drag effects at these lower altitudes. Currently, CubeSats are restricted to use at altitudes below 600 km due to the requirement to deorbit within 25 years [1]. Below 250 km, a CubeSat will last only a matter of hours due to the high drag force that the CubeSat would experience [2].

CubeSats have become increasingly popular for their low cost and short production time as compared to larger satellites. The most commonly used sizes of CubeSats are the 1U (10 cm × 10 cm × 10 cm), 3U (10 cm × 10 cm × 30 cm), and 6U (10 cm × 20 cm × 30 cm); the 6U is the largest CubeSat currently in orbit. The use of propulsion systems on CubeSats can be restricted or limited, based on the launch provider and the propellant type used. However, propulsion systems have the potential to decrease the orbit degradation at lower altitudes, and thus extend mission lifetime. These systems also enable orbit maneuvers, formation flying, orbit raising, and deorbiting. Larger CubeSats (6U, 12U, and 27U) are already being launched, and they will grow in use as more launch systems come online. These larger CubeSats provide a larger platform for a propulsion system to be implemented.

Research has been conducted over the past 15 years regarding air-breathing electric propulsion, which are sometimes referred to as atmosphere-breathing electric propulsion or ram-electric propulsion (RAM-EP). The primary application of interest for these systems is drag makeup and mission extension for extremely low Earth orbit (ELEO) satellites, i.e., systems in orbits below ~400 km, where drag limits typical CubeSat missions to about one year. Traditional propulsion systems could be used, but the amount of propellant that would have to be stored to extend the lifetime by any significant amount would be prohibitive. Instead of storing propellant, air-breathing thrusters use the tenuous neutral atmosphere in low Earth orbit (LEO) as propellant. The key advantage of such a concept is that the atmosphere, which is responsible for drag, is also used to produce thrust; the question to be addressed is whether a system can be designed and built where the thrust equals or exceeds drag at altitudes of interest.

In this paper, we investigate whether air-breathing systems are a viable option for CubeSats of 3U, 6U, 12U, and 27U sizes; and we design such a system with a focus on the inlet design and the calculations of achievable thrust. The thruster design is modular, such that larger components (e.g., the inlet) would be, at the most, 1U in size, as shown in Fig. 1a. Ann analysis is conducted on various inlet shapes in order to establish a particle capture efficiency, which is the number particles that reach the ionization stage of the thruster over the number of particles that enter the inlet. The ionization of atmospheric particles is also discussed, and the range of likely ionization efficiencies for this type of system is bounded. Using these efficiencies, we analyze the expected performance of this air-breathing micro-ion thruster. Figure 1b shows a mockup of the proposed system with key elements: 1) parabolic inlet, 2) ionization/ion confinement channel, and 3) acceleration grids and subsystems to the accelerator grids represented by the large cylinder. As with any electrostatic thruster system, a neutralizer would also need to be included, but that part of the system will not be discussed in this paper.

II. Background

A. Air-Breathing Research

In this section, we highlight several key air-breathing thruster concepts that are important and relevant to the current design. Conley proposed the idea of a deployable ionization chamber with acceleration grids in the mid-1990s [3], which was applicable to much larger spacecraft. The ionization chamber deploys from a large spacecraft operating at or below 200 km. The propulsion system was designed to be 5 m wide and 15 m in radius and use about 2.9 kW of

Received 6 June 2017; revision received 21 October 2017; accepted for publication 29 October 2017; published online 21 December 2017.

*M.S. Student, Ann and H.J. Smead Department of Aerospace Engineering Sciences.

†Assistant Professor, Ann and H.J. Smead Department of Aerospace Engineering Sciences.

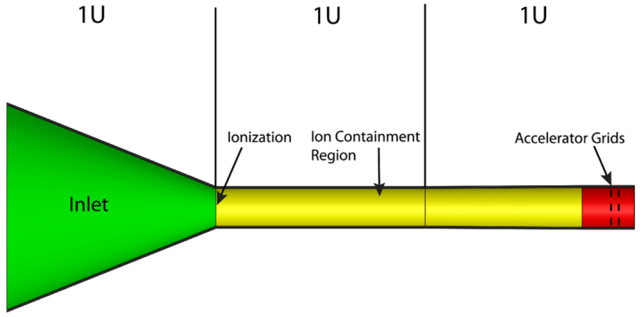

a)

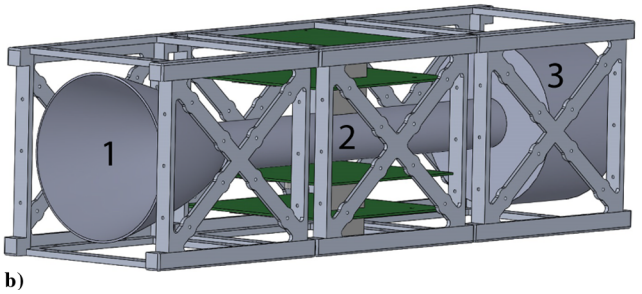

b)

Fig. 1 Representations of a) cross section and b) three-dimensional mockup of the proposed system.

power. The ambient neutral air molecules would be ionized by the satellite's trailing rings and then accelerated through the subsequent acceleration grids. Conley effectively proved that drag makeup using such a system was feasible at these altitudes; however, the size made his design infeasible for application. Conley understood this and suggested that, if slow ions could be contained in the "ionization cavity" with the circulating electrons, the density could be increased, thus allowing for a smaller more efficient thruster [3].

Around the same time, Nishiyama proposed the concept of an ion thruster with a similar methodology; however, instead of a deployable grid, the system would be attached on the outside of a satellite vehicle [4]. The proposed system would have long narrow tubes to capture the particles, and then it would have an electron cyclotron resonance microwave discharge to ionize the incoming particles before being accelerated through a grid. For this thruster, two critical assumptions were made. First, the thermal velocity of incoming particles was assumed to be much slower than the velocity of the space vehicle. Second, the mean free path of the particles was assumed to be much greater than the length of the inlet [5].

In contrast to Conley's passive capture approach [3], and as an alternative to Nishiyama's collimated capture method [4], a "scoop" collection concept was proposed by McGuire [6]. For this concept, it is assumed the given space vehicle is operating below 200 km and, more desirably, at 100 km. At these altitudes, the scoop must be modeled for use in the transition region where the flow goes from continuum to free molecular, and shocks forming at the front of the scoop must be taken into account [6]. McGuire's [6] and Nishiyama's [4] methods have competing views on the behavior of the flow; however, they both concluded that the smaller the inlet, the greater the capture percentage [5]. Although air-breathing thrusters are under development for CubeSats [7], there has yet to be an extensive analytical study on the subject until now.

B. Atmospheric Considerations

The neutral atmosphere in LEO impacts both the drag on the spacecraft as well as the available propellant to be used for thrust. As such, the atmospheric composition and density are important aspects of our design. This section highlights the key conditions in the atmosphere that will be essential to the analysis of the proposed system.

1. Atmospheric Composition

Earth's atmosphere extends to approximately 10,000 km above the Earth's surface. The atmosphere sees a number of key transitions at different altitudes due to the changing composition above a 100 km altitude. The density is also impacted by solar activity (F10.7) and geomagnetic activity Ap, which vary over an 11 year cycle. The atmosphere not only provides lift to aircraft, but it also works against lift by creating drag. For in-space propulsion, RAM-EP technology struggles with the tradeoff between altitude and efficiency. That is, the lower in altitude, the higher the density of the atmosphere, and therefore the more propellant that is available; however, this also means an increase in drag experienced by the space vehicle and a higher power requirement to produce the required thrust.

The altitude range of interest for this proposed system is between 80 and 600 km. Using the NRLMSISE-00 [8] atmosphere model, the particle density over the range of ELEO and LEO altitudes is plotted in Fig. 2a. Figure 2b shows the overall mass density variation with altitude for different solar conditions (see Table 1 [9]). Note, for Fig. 2a, that the values plotted are for an average solar flux ($f10.7 = 98.7$) and geomagnetic activity ($Ap = 8.6$) from 80 to 600 km for 0 deg latitude at 01:30 Universal Coordinated Time). At altitudes below ~125 km, Nitrogen (N_2) and Oxygen (O_2) will be the primary particles captured by the propulsion system and contributors to spacecraft drag. Argon will also contribute some for altitudes below 100 km but, above 100 km, its density drops off quickly, and thus argon is not considered in this study. As the altitude increases, there is an exponential decline in N_2 and O_2; at about 150 km, atomic

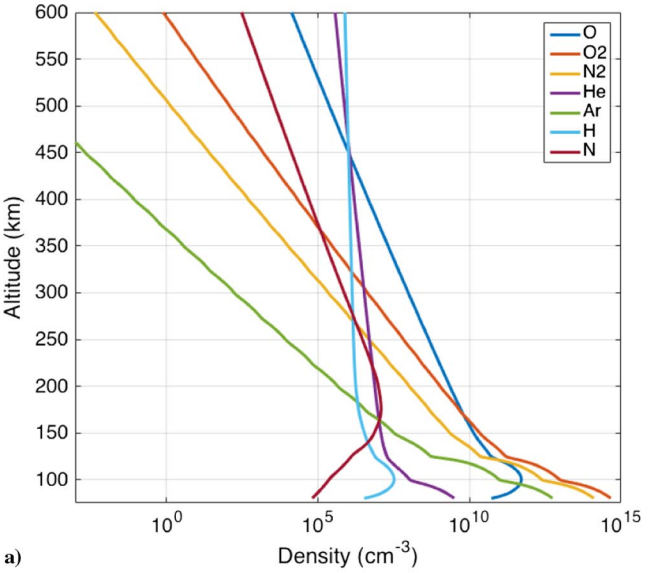

a)

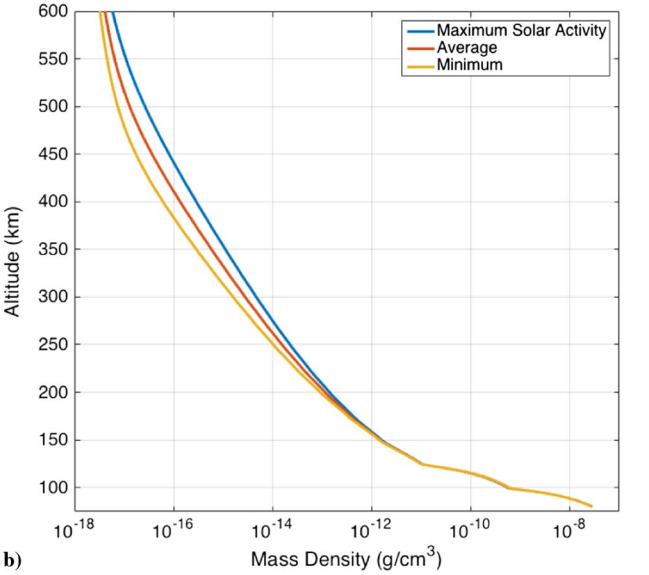

b)

Fig. 2 Representations of a) atmosphere particle density vs altitude and b) total mass density vs altitude.

Table 1 Solar and geomagnetic activity summary from 2005 to 2016 [9]

	Maximum	Average	Minimum
F10.7	145.5	98.7	68.2
Ap	15.1	8.6	3.8

oxygen becomes the dominant particle in the atmosphere. All other particle densities are too small to make a significant contribution to the system until about 450 km in altitude: above which, hydrogen and helium dominate the atmosphere's composition. This model is not only essential for determining how much propellant is available for the air-breathing system but also will allow for an accurate description of thrust available from each constituent of the atmosphere, as well as the drag that will be experienced by the system.

2. Orbit

The velocity of the spacecraft in orbit is a key parameter for estimating the thrust and drag on the system. All orbits are assumed to be circular, and the available propellant is assumed constant over the duration of an orbit. The density of the constituents will vary with latitude, longitude, and daylight/eclipse operations. This variation is small, but the atmospheric model data used assume operation in eclipse, which will underestimate the available propellant. A further performance analysis is necessary to take into account the effects of noncircular orbits, but that analysis is beyond the scope of this paper.

It is also important to quantify the speed at which the neutrals will enter the inlet of the system with respect to the space vehicle. Given that temperatures in the thermosphere range from ∼200 to 1000 K, depending on the observed constituents (oxygen, hydrogen, etc.), the maximum thermal velocity of any particle is around 3 km/s. According to McGuire [6], in LEOs, the thermal velocity of the neutrals and ions is anywhere between 500 and 1000 m/s at most. The spacecraft velocity in LEO is ∼7.7 km/s. Therefore, to simplify calculations, the relative velocity between the atmospheric particles and the spacecraft will be given by the spacecraft velocity for the purpose of both drag and thrust calculations, and particles are assumed to enter the inlet from the ram direction. This assumption limits this discussion to a single direction vector for all incoming neutrals, and it does not take into account variations in speed of the different constituents.

3. Drag

The drag force on an orbiting spacecraft is given by the following:

$$D = \frac{1}{2}\rho C_D A v^2 \tag{1}$$

The common standard drag coefficient used in most orbital mechanics calculations is $C_D = 2.2$. The value for C_D will also change for the portion of the flow ingested by the inlet; however, the variation has a small effect on the drag calculation as compared to that of density. The work of Pardini et al. [10] showed that, for altitudes below 450 km, a drag coefficient of $2.2 \pm 5\%$ was accurate for a comparable shape. According to Pardini et al. [10], there were two reasons why the drag coefficient increased at higher altitudes. First, the change in atmospheric composition (more helium and hydrogen atoms) led to lower accommodation values, which corresponded with higher drag coefficients. The second was due to a violation of the hyperthermal flow assumption. The thermal speed of the particles was higher at these higher altitudes, whereas the satellite's orbital velocity decreased. Therefore, despite variations that could occur with altitude, a coefficient of drag of 2.2 was a reasonable assumption for this analysis. Once the spacecraft was designed, C_D and A were set; only the mass density ρ and velocity v varied with altitude and time, and the latter only very weakly. Hence, ρ was the key parameter impacting drag on the spacecraft.

Is it important to note that this proposed system will operate in free molecular flow, which impacts how drag is calculated. In free molecular flow, the particle density is so small that, instead of being a fluid (i.e., a continuous stream of particles), each particle is viewed individually. In short, there is no interaction between the molecules; it is a collisionless environment. According to Vallado and Finkleman [11], accurately solving for drag under these conditions is complicated. Depending on which atmospheric model is used, the parameters of the satellite, the orbit in question, and the orbit propagation methods, the results can be varied. It is due to this fact that a free molecular flow drag model will not be implemented in this paper; however, for future analysis of this proposed air-breathing system for CubeSats, it may be necessary to construct such a model.

4. Gas–Surface Interactions

In free molecular flow, the interaction of a particle with a surface is important to characterize, especially when discussing the capture of particles in the inlet of RAM-EP systems. In the past 35 years, gas–surface interactions in space have been highly documented. This has led to the discovery that satellite surfaces are coated with "adsorbed" molecules that, in turn, affect the energy accommodation and reflection of molecules from the surface for satellites in the altitude range of 100–300 km [12]. The term adsorption refers to the trapping of atomic oxygen and its reaction products on the satellite's surface. If the surface is clean, or devoid of trapped atoms and molecules, incoming particles will reflect nearly specularly. However, as the surface becomes contaminated with adsorbed atoms and molecules, the incoming particles are reflected more diffusely and, in turn, lose a large portion of their incident kinetic energy [12]. As altitude increases, the surface coverage of adsorbed atoms and molecules decreases. Referring back to Fig. 2a, this should be of no surprise because we see that the atomic oxygen density is almost five orders of magnitude smaller above 300 km than at its peak near 100 km.

Therefore, the reflections that occur from satellite surfaces will be quasi specular in nature while the surface is not full contaminated. As the contamination is increased, the fraction of quasi-specular reflections decreases and the diffuse fraction of reflections increases. Figure 3 shows a representation of the quasi-specular reflection. In our calculations, we take into account the full range of conditions from fully diffuse to fully specular reflections to investigate the range of particle capture efficiency.

C. Thrust Equations

According to Goebel and Katz [13], the thrust for an electric propulsion system is given by the following:

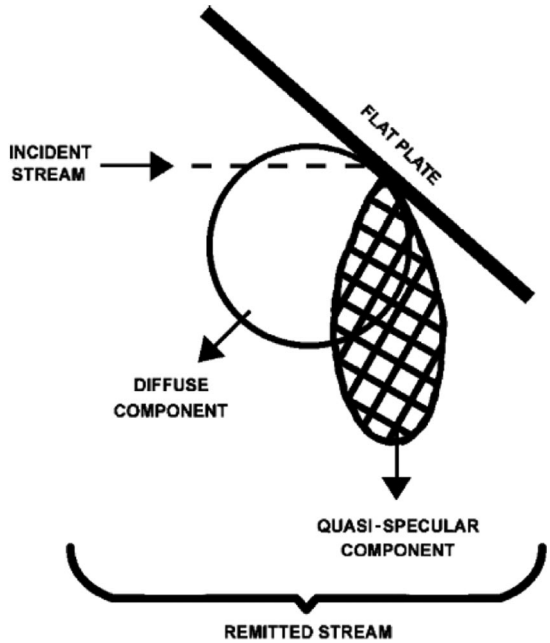

Fig. 3 Drawing showing that, off of a surface not fully contaminated, the reflection will be quasi-specular.

$$T = \sqrt{\frac{2m_i}{q}} I_b \sqrt{V_b} \tag{2}$$

where the beam current (i.e., the current of ionized particles at the entrance to the grid gap) is given by the following:

$$I_b = \frac{1}{2} n_i q v_a A T_g \tag{3}$$

The acoustic velocity will only apply in high-density flows; therefore, to account for this variable, the velocity of the ions through the grid gap is determined. Equation (4) shows the equation of motion in terms of the charge and the electric field, which can be integrated with respect to time in order to get the time for a single ion to cross the grid gap:

$$d = \iint \frac{q\boldsymbol{E}}{m_i} \, \mathrm{d}t^2 \tag{4}$$

where d is the known grid gap distance, and $\boldsymbol{E}$ is the electric field. The velocity through the grid gap is then

$$v_g = \frac{qV_b}{m_i d} t \tag{5}$$

In the case of an air-breathing system, the thrust and drag will primarily vary as density varies. As shown in Eqs. (1) and (6), this relationship is linear. To see this, we can rewrite the equation for thrust in terms of density:

$$T = \sqrt{\frac{q}{2m_i}} \rho v_g A T_g \sqrt{V_b} \tag{6}$$

Referring back to Eq. (1), the thrust to drag ratio T/D is given by the following:

$$\frac{T}{D} = \frac{\sqrt{(q/2m_i)} v_g A T_g \sqrt{V_b}}{(1/2) C_D A v^2} = C_1 \sqrt{\frac{1}{m_i}} \left(\frac{1}{v^2} \right) \tag{7}$$

where the constant C_1 depends only on the physical constants and parameters of the spacecraft and propulsion system design (C_D, A, T_g, and V_b). This relationship shows that T/D depends only on the atmospheric composition, through m_i, and the spacecraft orbital velocity, which varies only weakly with altitude. As such, we expect T/D to be relatively constant with altitude, changing primarily with the atmospheric composition.

In this system, the ram drag must also be taken into account. This is the same effect that occurs on turbofan engines. Ram drag is produced by a velocity differential between the incoming particle velocity and the velocity of the particles at the exit of the system. The thrust will therefore be reduced by a factor of

$$\epsilon_{\text{ram}} = \frac{g_0 I_{\text{sp}} - v_{\text{rel}}}{g_0 I_{\text{sp}}} \tag{8}$$

where v_{rel} is defined as the orbital velocity:

$$v_{\text{rel}} = \sqrt{\frac{\mu}{R_e + h}} \tag{9}$$

where μ is the gravitational constant of the Earth, R_e is the radius of the Earth, and h is the altitude of the spacecraft.

III. Design

Equation (2) for the thrust is modified by three efficiencies determined by the design of the system. The first efficiency is the particle capture efficiency, given by the fraction of incoming neutrals that make it to the ionization stage of the thruster. The second efficiency is the ionization efficiency, i.e., the fraction of particles that are ionized and thus available for thrust. The third efficiency is the ram drag efficiency in Eq. (8). Accounting for these efficiencies, Eq. (2) is now given by the following:

$$T = \eta_c \eta_u \epsilon_{\text{ram}} \sqrt{\frac{2m_i}{q}} I_b \sqrt{V_b} \tag{10}$$

Note that the grid transparency and ionization efficiency were combined into one term n_u for the purposes of this discussion.

A. Inlet

According to Singh and Walker [5], current inlet designs have capture efficiencies below 50%, with the two most prominent designs being Nishiyama's collimated inlet [4] and McGuire's conical scoop [6]. In an attempt to find a better design, we chose to test particle capture with different geometric shapes. We tested three different shapes for their effectiveness in capturing incoming particles. A pyramidal shape, a conical shape, and a parabolic shape were each tested with a feasible length, given that this inlet will fit inside a 1U volume (shown in Figs. 4a–4c).

The MolFlow+ software developed by Kersevan and Pons [14] is used to the run the analysis on these three shapes. MolFlow+ uses what is referred to as the "test-particle Monte Carlo" algorithm in order to model rarefied gas flow. MolFlow+ is capable of modeling specular and diffuse reflections, and diffuse reflections can be specified with cosine or uniform distributions. The analysis in this paper shows simulation under specular and diffuse conditions. A cosine distribution is used in order to simulate a straight flowpath into the inlets.

We tested the inlets shapes with three different lengths: 5, 7.5, and 10 cm. It was assumed that the temperatures of all the surfaces were uniform. The pyramidal inlet with a length of 10 cm has an inlet area of 10 by 10 cm and an outlet area of 2 by 2 cm. The conical inlet (similar to McGuire's scoop [6]) with a length of 10 cm has an inlet

a) b) c)

Fig. 4 Cross sections of the test inlet shapes: a) pyramidal inlet, b) conical inlet, and c) parabolic inlet.

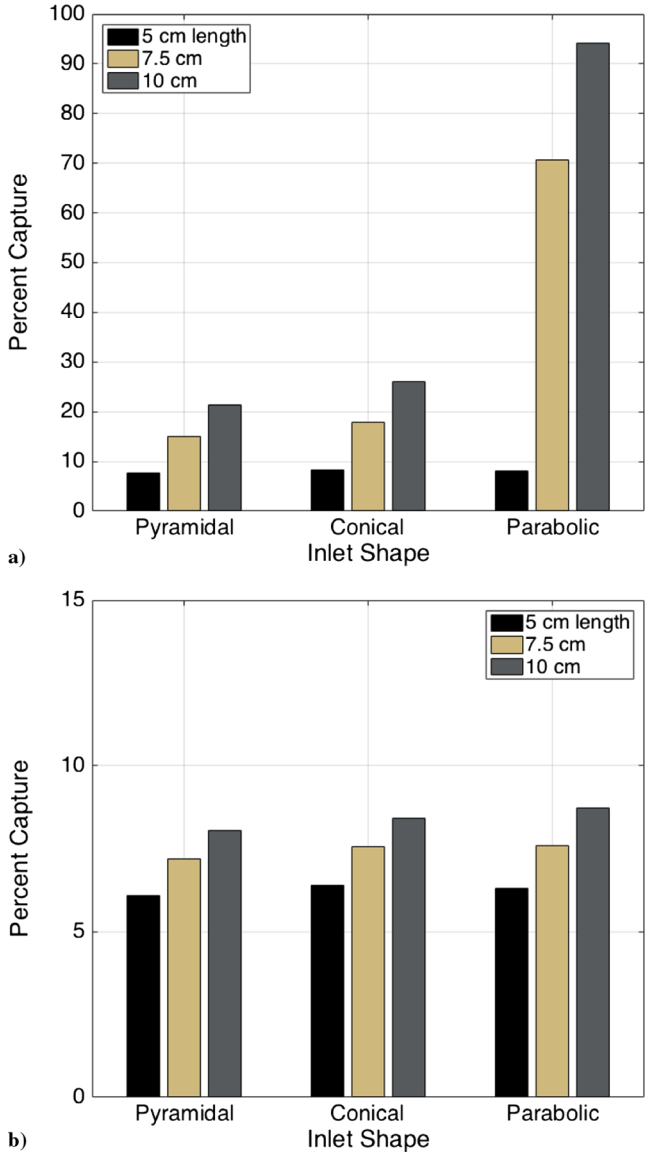

Fig. 5 Inlet capture percentage for various inlet lengths with a) specular particle reflections and b) diffuse particle reflections.

radius of 5 cm and an exit radius of 1 cm. The parabolic inlet with a 10 cm length has a 5 cm inlet radius and a 1 cm exit radius.

The results of the MolFlow+ analysis are shown in Figs. 5a and 5b. Under the ideal scenario of specular reflection, it is clear that the parabolic shape outperforms the other two shapes due to the optics of a parabola; all particles will reflect toward the focus of the parabola. The capture percentage of the parabolic shape is not 100% due to the dimensions of the parabola. To make the inlet fit within a 1U volume, the dimensions are such that the focus is designed to be just in front of the outlet. The results for the conical shape are well below 50% capture, as expected according to the literature review conducted by Singh and Walker [5].

Under diffuse conditions, the inlets' performances are nearly identical. Due to the random nature of the reflections from the surface, this is no surprise. However, at the longer length of 10 cm, the parabolic shape has a slightly greater capture percentage. From these results, we conclude that a 10 cm length and a parabolic inlet shape are the best choice for further analysis. In the work of Jackson [15], the inlet design was further explored and a unique method to increase the capture efficiency under diffuse conditions was proposed.

Figure 6 shows the quasi-specular range that can be obtained, based on the data from the specular and diffuse analysis of the inlets. We determined from this analysis that a range for the particle

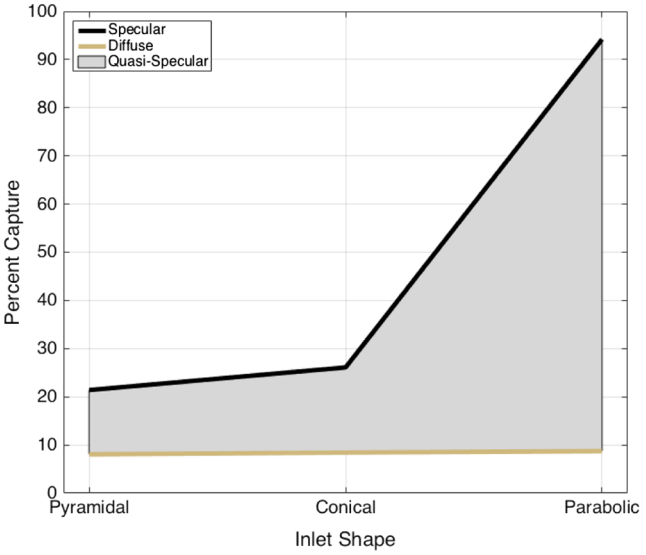

Fig. 6 Quasi-specular region of efficiency for different inlet shapes.

capture efficiency would be between roughly 10 to 90% using the parabolic inlet.

B. Ionization

Once the neutral particles have been collected and funneled into the system, they must be ionized to be useful as propellant. In this section, we provide a basic overview of the state of research and the range of possible ionization efficiencies for a proposed air-breathing CubeSat thruster. The primary issues with selecting a plasma generator lie within current technological limitations. Traditional thermionic cathode emission sources operate well within noble gases [5] and less commonly within oxygen-containing gases. A nonthermionic emission source prototype has been designed, but it has not been developed or tested. As far as RF or microwave cathodes, no tests have been conducted on atmospheric constituents [5].

Although current ionization methods are capable of high efficiencies for xenon, the results are not directly translatable to atmospheric constituents [5]. According to Wirz et al. [16], a micro-ion thruster of comparable size to the one that would be used in our proposed system has an ionization efficiency of 50% (as high as 82%) using a dc discharge system. However, according to Pilinski [17], the dc discharge ionization efficiency for neutral atmospheric particles is much lower. The Drag and Atmospheric Neutral Density Explorer (DANDE) satellite was designed to ingest and ionize neutral atmospheric particles for atmospheric composition analysis. The research on DANDE showed that the expected ionization efficiency for these low-density neutral particles was 0.1% [17]. On the other hand, Shabshelowitz [18], whose research focused specifically on ionization for air-breathing thrusters using RF discharge, made an estimate of 10% ionization efficiency. A white paper by Matney [19] that based its work on Conley [3] was optimistic that 100% ionization of the incoming particles was possible, given the proper chamber design.

In the work of Shabshelowitz [18], the conclusion was that an RF plasma generator can increase ionization for a Hall-effect thruster thruster and, even though air-breathing propulsion is feasible for smaller satellites, there needs to be further study of the ionization of the atmospheric constituents. In general, the ionization of atmospheric gases for use in electrostatic thrusters will require further research before a consensus can be reached on ionization efficiencies. It is possible that new methods of ionization might need to be explored in order for the atmospheric constituents to reach the same efficiencies as xenon propellant [5]. For this research, we assume a 10% ionization efficiency, but an analysis of how ionization impacts the performance of this proposed system is explored in the next section, in which we vary the ionization efficiency from 0.1 to 50%.

IV. Analysis

A. Setup

Having established the inlet's particle capture efficiency range and the expected ionization efficiency, we characterized the thrust for this proposed air-breathing system. The concept thruster was analyzed for 3U, 6U, 12U, and 27U standard CubeSat form factors. The following performance characteristics and assumptions were made unless otherwise noted:

1) The proposed electric thrust was power limited to 10 W.

2) A beam voltage of 700 V was used. The beam voltage and total voltage were considered equal because the number of particles affecting the electric field were small. This number was considered a good estimate of performance, based on similar systems [16].

3) The average F10.7 and Ap were used, based on the last 11 years.

4) The 3U, 6U, 12U, and 27U CubeSats dimensions were as follows: 3U was $0.10 \times 0.10 \times 0.30$ cm, 6U was $0.12 \times 0.24 \times 0.36$ cm, 12U was $0.24 \times 0.24 \times 0.36$ cm, and 27U was $0.34 \times 0.35 \times 0.35$ cm.

5) All drag calculations were conducted for the smallest CubeSat face in the ram direction (i.e., the direction of orbital velocity).

6) The system was assumed to be ionizing a combination of atomic oxygen, O_2, N_2, and hydrogen.

7) The number of inlets used was based on the size of the CubeSat being analyzed. This directly impacted the density of the available propellant, and therefore the thrust.

8) The conservation of mass was used to estimate the density at the outlet aperture of the inlet. That is,

$$\rho_1 A_1 \psi = \rho_2 A_2 \psi \tag{11}$$

where any loss in speed experienced by the incoming neutrals interacting with the wall or reflected particles was assumed to be negligible, such that the velocity was constant across the length of the inlet. This simplifying assumption was justified by the fact that the mean free path showed that the collisions would be few due to the density of the constituents. Also, the interactions with the wall were most severe in the diffuse case, and a majority of the particles, despite their change in speed in reality, would be reflected back out of the inlet.

9) The ionization efficiency was 10%.

B. Thrust Analysis

1. *Particle Contribution*

We analyze the contributions of the individual constituents to thrust first. We assume a simple 3U system shown in Fig. 1b without power limitations. Figure 7 shows the results of this analysis by assuming 90% inlet efficiency; the thrust scales linearly with this efficiency. We observe that the overall thrust follows asymptotes bounded by hydrogen above approximately 450 km, atomic oxygen between 175 and 450 km, and N_2 below 175 km. Clearly, at higher LEO orbits, hydrogen will be the primary contributor to thrust; at lower altitudes, the system can rely on N_2 and O_2. The small anomalies seen at the lower altitudes are due to jumps in overall atmospheric density below 125 km.

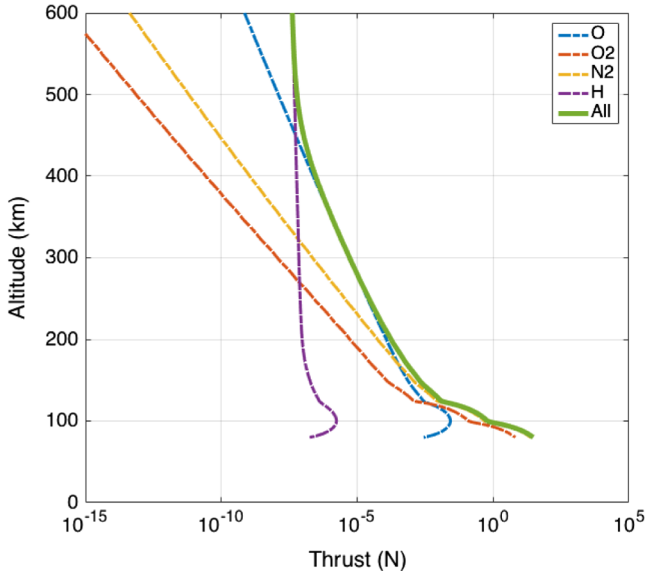

Fig. 7 Particle contribution to thrust at various altitudes at 90% inlet efficiency for a 3U system.

2. *Solar Activity*

Solar activity will affect the particle density of the atmosphere that, as shown in Eq. (6), will affect thrust. An analysis of this effect is examined at 125 and 300 km orbits for maximum and minimum inlet efficiencies, assuming an operating voltage of 700 V and a non-power limited system. Figures 8a and 8b show the thruster performance of a

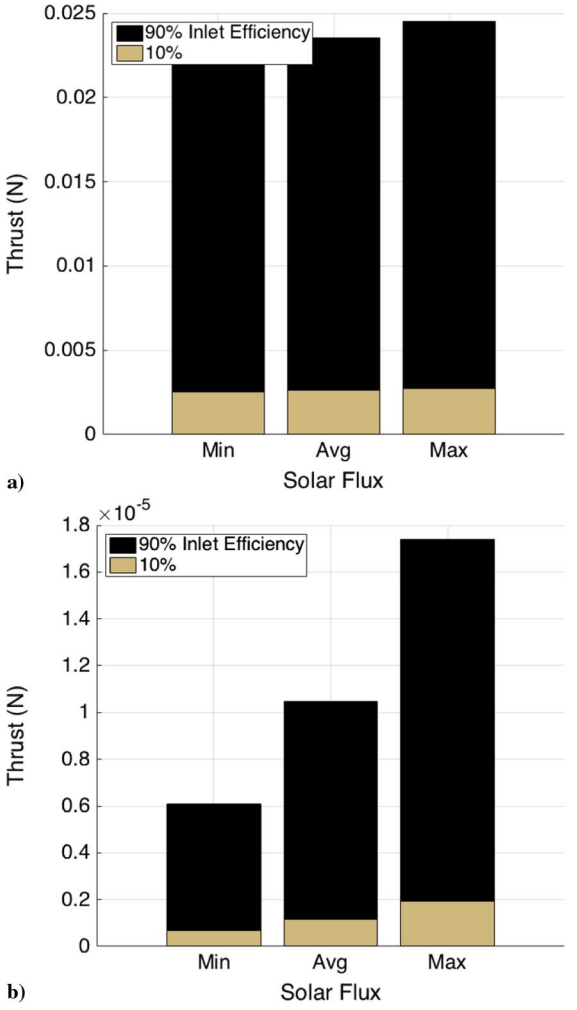

Fig. 8 Thrust at maximum (Max), minimum (Min), and average (Avg) solar activity for a 6U system at a) 125 km and b) 300 km.

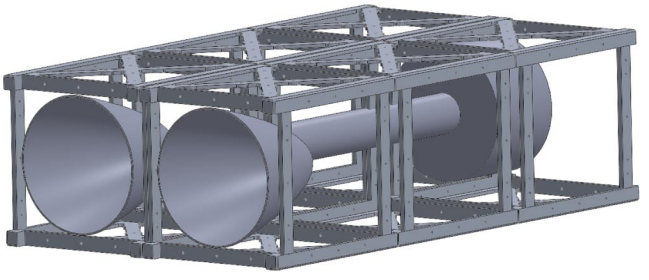

Fig. 9 Mockup of the 6U-sized thruster system.

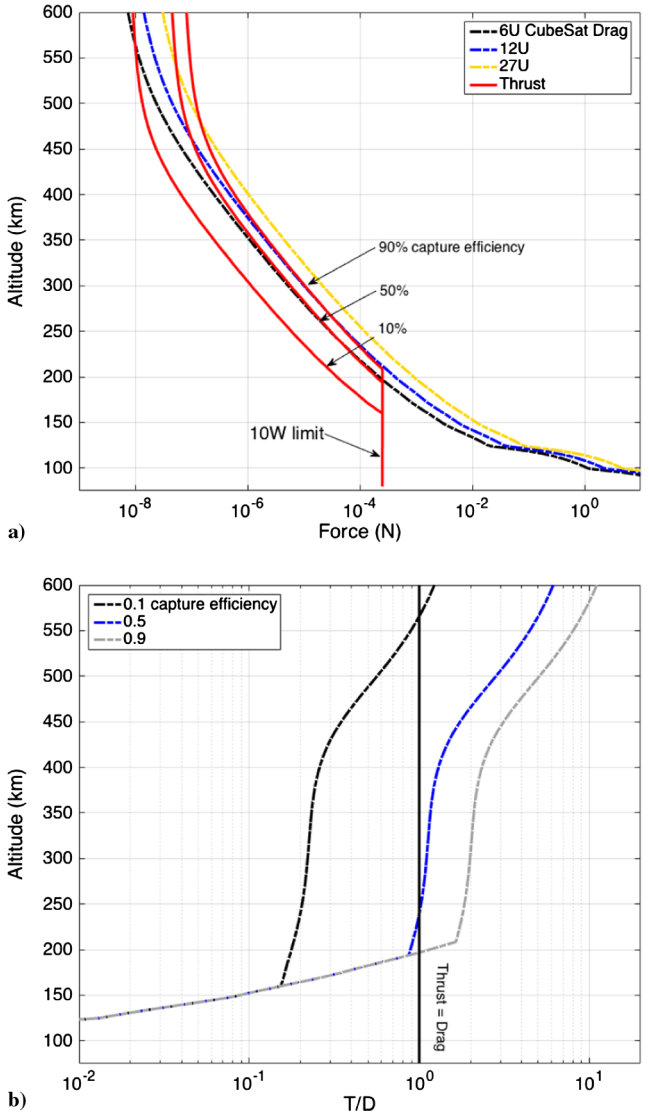

Fig. 10 Representations of a) thrust versus drag and b) thrust-to-drag ratio for 10, 50, and 90% inlet capture efficiencies for a 6U system.

6U CubeSat (with two inlets as shown in Fig. 9 varying with solar flux at 125 and 300 km). Table 1 summarizes the values used for F10.7 and Ap for maximum, minimum, and average solar activity.

At the lower altitudes, the solar flux has little impact on the overall thrust, which is directly correlated to the density remaining fairly consistent with variations in the solar flux at these altitudes. The real difference is experienced at higher altitudes (as shown in Fig. 2b), and the difference in the thrust increases between the solar maximum and the solar minimum as the altitude increases. At an altitude of 300 km, the thrust is already an order of magnitude different between the minimum and maximum solar fluxes. These results similarly apply to the 12U and 27U CubeSats [15].

3. *Thrust Versus Drag*

The quintessential question to be answered via this paper is whether the thrust of this system can overcome drag and, if so, at what altitudes. Figures 10a and 10b show the thrust compared to drag for a 6U CubeSat configuration that would use two inlets feeding into one ion thruster. Figure 10a shows the thrust of a 6U system with inlet efficiency varying from 10 to 90% with a power limit of 10 W, and Fig. 10b shows the thrust-to-drag ratio for the same system at inlet efficiencies of 10, 50, and 90%.

For the 6U system, the thruster matches drag above about 200 km for inlet efficiencies above 50%. For the 12U and 27U thruster systems, the thrust matches drag between 200 and 250 km for inlet efficiencies above about 50% [15]. The larger system, such as the 12U and 27U CubeSats, experiences more drag but has room for more inlets and/or a full thruster system to counteract the increase in drag.

4. *Thrust Versus Ionization Efficiency*

The currently limited research into ionization of atmospheric particles has not provided a definitive value for the ionization efficiency of these particles. In fact, it may be possible that new technology needs to be developed in order to efficiently ionize atmospheric particles in the upper atmosphere. This section will therefore analyze and discuss the effect that the ionization efficiency has on the performance of this proposed system. Here, we consider the 6U CubeSat design with an operating voltage of 700 V; and we will vary the inlet capture efficiency between 10, 50, and 90%. The performance is analyzed at ionization efficiencies of 0.1, 1, 10, and 50%.

Figure 11 shows the thrust versus drag for 0.1, 1, 10, and 50% ionization efficiency. For the 0.1 and 1% cases, the thruster is no longer a viable drag makeup solution for LEO orbits. The efficiency of the inlet is a significant factor of the thruster's performance until the system reaches lower altitudes where more power is required to operate partially due to the increase in the density of constituents. The line at which all of the efficiencies converge shows the altitude where the inlet efficiency becomes insignificant and the power limitation of the system dictates performance. At 10% ionization efficiency (the same as Fig. 10b), the thruster is only effective above 200 km for drag makeup if the inlet is capable of at least 50% particle capture. At 50% ionization efficiency, the system is able to produce thrust exceeding drag for a worst-case capture efficiency of 10%, as well as for all altitudes above 200 km.

For ionization efficiencies between 10 and 50%, it can be seen that the inlet capture efficiency becomes an important factor in the thruster's ability to overcome drag. If the thruster is able to ionize as well as the Miniature Xenon Ion (MiXi) thruster by Wirz [20] (50% ionization efficiency), the thruster will be effective from 225 to 600 km in altitude. For ionization efficiencies greater than 50%, the thruster will be able to overcome drag, but the power will limit the altitude at which the thrust exceeds drag. Below a 10% ionization efficiency, this proposed thruster design will be entirely incapable of overcoming drag in LEO orbits.

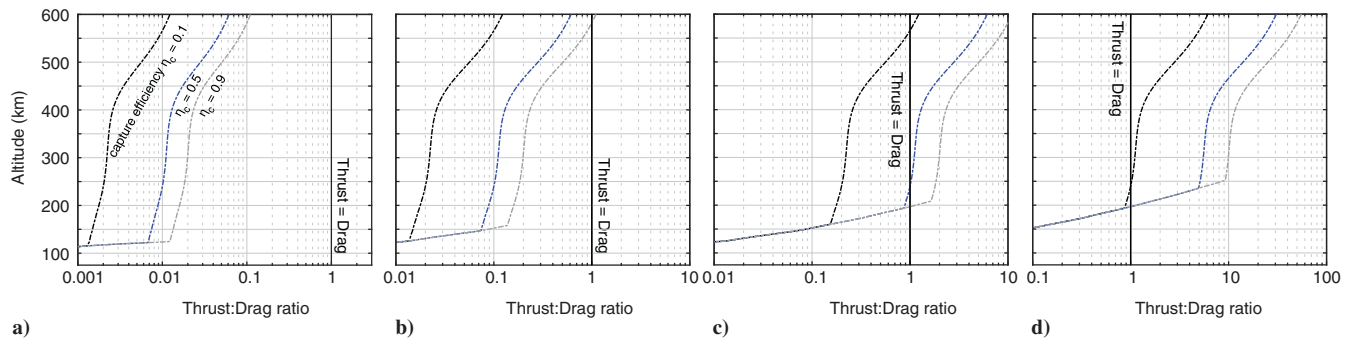

Fig. 11 Thrust-to-drag ratio for a 6U CubeSat for various ionization efficiencies: a) 0.1% ionization efficiency, b) 1%, c) 10%, and d) 50%.

V. Conclusions

The results show that the ionization efficiency is crucial to the thruster's ability to overcome drag in low Earth orbit (LEO). A 3U version of this system will only be able to match drag above approximately 300 km if the combined efficiency of the inlet and ionization is greater than or equal to 9%. The 6U, 12U, and 27U systems configurations are capable of counteracting drag at 200 km if the combined efficiency of the inlet and ionization remains roughly at or above 5%.

If the ionization efficiency is 50%, the performance is greatly improved with the 6U system capable of matching drag at ∼200 km with only 10% inlet efficiency. If the ionization efficiency is less than or equal to 1%, the thruster becomes unable to counteract drag in LEO orbits, and is therefore not a viable solution for CubeSat applications.

It is believed that this proposed system shows promise as an air-breathing electric CubeSat thruster; however, this is strictly dependent upon the ionization efficiency of the plasma generator and the contamination rate of the inlet surface. Further research into ionization of atmospheric particles will determine if this system truly is a viable CubeSat propulsion system.

References

[1] Inter-Agency Space Debris Coordination Committee, "IADC Space Debris Mitigation Guidelines," IADC-02-01, 2007, http://www.iadc-online.org/Documents/IADC-2002-01,%20IADC%20Space%20Debris%20Guidelines,%20Revision%201.pdf [retrieved 2017].

[2] Oltrogge, D. L., and Leveque, K., "An Evaluation of CubeSat Orbital Decay," *25th Annual AIAA/USU Conference on Small Satellites*, Analytical Graphics Inc., SSC11-VII-2, Colorado Springs, CO, SRI Inc., Menlo Park, CA, 2011.

[3] Conley, B. R., "Utilization of Ambient Gas as a Propellant for Low Earth Orbit Electric Propulsion," M.S. Thesis, Massachusetts Inst. of Technology, Cambridge, MA, 1995.

[4] Nishiyama, K., "Air Breathing Ion Engine Concept," *54th International Astronautical Congress of the International Astronautical Federation, the International Academy of Astronautics, and the International Institute of Space Law*, AIAA, Reston, VA, 2003. doi:10.2514/6.iac-03-s.4.02

[5] Singh, L. A., and Walker, M. L., "A Review of Research in Low Earth Orbit Propellant Collection," *Progress in Aerospace Sciences*, Vol. 75, 2015, pp. 15–25. doi:10.1016/j.paerosci.2015.03.001

[6] McGuire, T. J., "Aero-Assisted Orbital Transfer Vehicles Utilizing Atmosphere Ingestion," M.S. Thesis, Massachusetts Inst. of Technology, Cambridge, MA, 2001.

[7] Voss, H., Dailey, J., Bauson, W., and Chapman, B., "Nano-Satellites and HARP for Student Learning and Research," *2015 ASEE Annual Conference and Exposition Proceedings, ASEE Conferences*, 2015. doi:10.18260/p.24518

[8] Picone, J. M., Hedin, A. E., Drob, D. P., and Aikin, A. C., "NRLMSISE-00 Empirical Model of the Atmosphere: Statistical Comparisons and Scientific Issues," *Journal of Geophysical Research: Space Physics*, Vol. 107, No. A12, 2002, pp. SIA 15-1–SIA 15-16. doi:10.1029/2002JA009430

[9] "Recent Solar Indices" [online database], U.S. Dept. of Commerce, National Oceanic and Atmospheric Administration, 2017, ftp://ftp.swpc.noaa.gov/pub/weekly/RecentIndices.txt [retrieved 25 Jan. 2017].

[10] Pardini, C., Tobiska, W. K., and Anselmo, L., "Analysis of the Orbital Decay of Spherical Satellites Using Different Solar Flux Proxies and Atmospheric Density Models," *Advances in Space Research*, Vol. 37, No. 2, 2006, pp. 392–400. doi:10.1016/j.asr.2004.10.009

[11] Vallado, D., and Finkleman, D., "A Critical Assessment of Satellite Drag and Atmospheric Density Modeling," *AIAA/AAS Astrodynamics Specialist Conference and Exhibit*, AIAA Paper 2008-6442, 2008. doi:10.2514/6.2008-6442

[12] Moe, K., and Moe, M. M., "Gas–Surface Interactions and Satellite Drag Coefficients," *Planetary and Space Science*, Vol. 53, No. 8, 2005, pp. 793–801. doi:10.1016/j.pss.2005.03.005

[13] Goebel, D. M., and Katz, I., *Fundamentals of Electric Propulsion*, Wiley, Hoboken, NJ, 2008, pp. 33–34. doi:10.1002/9780470436448

[14] Kersevan, R., and Pons, J.-L., "Introduction to MOLFLOW: New Graphical Processing Unit-Based Monte Carlo Code for Simulating Molecular Flows and for Calculating Angular Coefficients in the Compute Unified Device Architecture Environment," *Journal of Vacuum Science and Technology A: Vacuum, Surfaces, and Films*, Vol. 27, No. 4, 2009, pp. 1017–1023. doi:10.1116/1.3153280

[15] Jackson, S. W., "Design of an Air-Breathing Electric Thruster for CubeSat Applications," M.S. Thesis, Univ. of Colorado Boulder, Boulder, CO, 2017. doi:10.13140/RG.2.2.34587.57124

[16] Wirz, R., Polk, J., Marrese, C., Mueller, J., Escobedo, J., and Sheehan, P., "Development and Testing of a 3 cm Electron Bombardment Micro-Ion Thruster," *International Electric Propulsion Conference*, Jet Propulsion Lab., IEPC-01-343, Pasadena, CA, 2001.

[17] Pilinski, M., "Analysis of a Novel Approach for Determining Atmospheric Density from Satellite Drag," M.S. Thesis, Univ. of Colorado Boulder, Boulder, CO, 2008.

[18] Shabshelowitz, A., "Study of RF Plasma Technology Applied to Air-Breathing Electric Propulsion," Ph.D. Thesis, Univ. of Michigan, Ann Arbor, MI, 2013.

[19] Matney, M., "An Electric Propulsion "Shepherd" for Active Debris Removal that Utilizes Ambient Gas as Propellant," *64th International Astronautical Congress*, NASA Johnson Space Center, JSC-CN-28296, Houston, TX, Sept. 2013.

[20] Wirz, R. E., "Miniature Ion Thrusters: A Review of Modern Technologies and Mission Capabilities," *Joint Conference of 30th ISTS, 34th IEPC and 6th NSAT*, Univ. of California, IEPC-2015-275/ISTS-2015-b-275, Los Angeles, CA, 2015.

M. L. R. Walker
Associate Editor